Evaluation of Large Eddy Simulation and Euler-Euler CFD Models for Solids Flow Dynamics in a Stirred Tank Reactor

Debangshu Guha, P. A. Ramachandran, and M. P. Dudukovic
Chemical Reaction Engineering Laboratory, Dept. of Energy, Environmental and Chemical Engineering, Washington University, St. Louis, MO 63130

J. J. Derksen
Multi-Scale Physics Dept., Delft University of Technology, Delft, The Netherlands

DOI 10.1002/aic.11417
Published online January 25, 2008 in Wiley InterScience (www.interscience.wiley.com).

Mechanically agitated reactors find wide range of applications for solid suspension and mixing in the chemical, biochemical, and mineral processing industries. Understanding the solids dynamics in these reactors is necessary to improve the design and operation of such reactors. Computational fluid dynamic (CFD) models are often useful in this regard, as it can provide significant insights into the flow and mixing of the phases involved. However, the model predictions need extensive evaluation with experimental results before they can be confidently used for the scale-up and optimization of large scale reactors. Recently, Guha et al. carried out a systematic experimental investigation of the solids hydrodynamics in dense solid–liquid suspensions (2.5–19% solids loading w/w) in a stirred tank using the Computer Automated Radioactive Particle Tracking (CARPT) technique, which provided extensive information to efficiently assess the ability of the existing CFD models in predicting the solids dynamics in slurry reactors. This work presents such an evaluation by comparing the averaged solids velocities, turbulent kinetic energy, and solids sojourn time distributions predicted by CFD models with those obtained from the CARPT experiment for overall solids holdup of 1% (v/v) (2.5% w/w) at Reynolds number of 74,000. The Large Eddy Simulation (LES) and the Euler-Euler model are the models chosen for evaluation in the current study. © 2008 American Institute of Chemical Engineers *AIChE J,* 54: 766–778, 2008
Keywords: solid-liquid, stirred tank, large Eddy simulation, Euler-Euler, CFD

Introduction

Slurry reactors, in which solid–liquid suspensions are agitated using one or more impellers, are one of the most important unit operations in the chemical, biochemical, and mineral processing industries, because of its ability to provide excellent mixing between the phases. The flow pattern and turbulence prevailing in the reactor ensures good heat and mass transfer properties for the system, apart from providing good solid suspension within the vessel. Relevant examples of solid–liquid industrial systems include multiphase catalytic reactions, crystallization, precipitation, leaching, dissolution, coagulations, and water treatment. Despite its widespread use, the design and operation of these reactors still remain a challenging problem because of the complexity of three dimensional circulating and turbulent multiphase flow encountered in the tanks.

Correspondence concerning this article should be addressed to M. P. Dudukovic at dudu@seas.wustl.edu.

With the improvement in computational capabilities, computational fluid dynamics (CFD) has emerged as a viable option to study turbulent multiphase flows and gain insights on the hydrodynamic behavior of complex systems. Several such attempts have been made to investigate the solids flow dynamics in stirred tank reactor as well, starting from the "black-box" approach to describe the impeller,[1,2] where experimental data provides the boundary conditions at the impeller region to perform the simulation. The "black-box" approach is obviously not entirely predictive in nature and requires experimental information at all conditions that are simulated. The increase in computational power further leads to the use of Algebraic Slip Mixture model[3] which assumes that both the phases exist at all points in space in the form of interpenetrating continua, and the equations solved comprise of the continuity and momentum equations for the mixture, volume fraction equation for the secondary phase and an algebraic equation for the slip velocity between the phases which then allows the two phases to move at different velocities. The Euler-Euler approach also invokes the concept of interpenetrating continua, but solves the continuity and momentum balances for each phase separately which results in simultaneous determination of the flow fields of the two phases.[4–9] The Euler-Lagrange approach, on the other hand, considers each particle individually and tracks their trajectories by solving the equations of motions for each of them.[10,11] As a result, this approach is considerably more expensive compared with the Euler-Euler approach and is mostly limited to simulations of solids volume fraction less than about 5%. Derksen[12] used the large eddy simulation (LES) to model the solids hydrodynamics in a turbulently agitated stirred tank. The LES methodology is much more fundamentally based compared with that of the standard RANS based models since it directly solves for the large scale eddies while the influence of the small scale eddies on the flow are modeled. The rationale behind LES is based on the fact that the smaller scales in the energy cascade are largely passive taking up whatever energy is passed on to them from the larger scales, which is justified since energy and information generally travel down to smaller scales, but not in the reverse direction.[13] LES has been successfully applied to model single phase flows in stirred vessels[14] and comparison with RANS simulation and LDA data[15] clearly demonstrates the superiority of LES in terms of predicting the turbulent quantities in the reactor. However, it should be noted that the improvement in the predictions obtained in a large eddy simulation is at the expense of the computational cost associated with it. As a result these simulations are still limited to smaller reactor sizes and relatively lower volume fractions of solids.[12] The most fundamental simulation that can be carried out is the direct numerical simulation (DNS), where the effect of eddies on the flow are not modeled at any scale and eddies of all sizes from the largest (order of reactor length scale) to the smallest (Kolmogorov microscale) are computed directly. Sbrizzai et al.[16] attempted to carry out a direct numerical simulation of the solids dispersion in an unbaffled stirred tank reactor, where the Lagrangian tracking of the solids were performed only for the period of three impeller revolutions because of the limitations of computational resources. However, the authors observed that this time window was not long enough to obtain a fully developed field for the solids phase, and hence they used their preliminary study only to derive an understanding on the transient dispersion dynamics. Considering the facts that often (though not always) it is the large scale eddies which are dominant, and that in DNS most of the computational effort is spent in resolving the small-to-intermediate scales,[13] large eddy simulation becomes the more viable option compared with DNS to gain fundamental understanding on two-phase turbulent flows.

Although computational fluid dynamics (CFD) does provide a platform that can be used to obtain significant insights into complex multiphase flow problems, it is essential to validate the model predictions with experimental data before they can be confidently used for the design and operation of industrial reactors. However, most of the experimental work carried out for solid–liquid stirred tanks focuses on the determination of the minimum impeller speed for incipient particle suspension[17–20] resulting in correlations which are similar to that of Zwietering's[21] except that variations in the exponents of different terms can be observed. Although the available correlations in the literature have significant importance from an operational point of view, they do not provide a clear understanding of the physics underlying the system. The experimental studies reported in the literature mostly consists of the axial measurement of concentration profiles in the vessel,[8,22–25] which ignore the radial gradients that exist in the reactor. As a result, the majority of the CFD studies for solid–liquid stirred tanks are either devoted to the improved prediction of axial solid concentration profiles only,[2,3,7–9,26] or are focused on the prediction of particle suspension height in a stirred vessel.[6] On the other hand, only few attempts can be found in the open literature to experimentally quantify the solids flow field in a slurry reactor. Nouri and Whitelaw[27] used the laser-Doppler velocimetry (LDV) to obtain the mean velocities and turbulent quantities of the solid phase in a Rushton turbine driven fully baffled stirred tank where the suspension was predominantly very dilute (0.02 v/v). This is well below 0.3% suggested by Lumley (1978) for particle–particle interaction to be significant, and hence, the reported solid hydrodynamics does not show very significant deviation from the measurements obtained for single phase flow.[27] The Lagrangian tracking of a solid particle inside a stirred tank using two synchronized video cameras by Wittmer et al.[28] cannot be considered a versatile technique because of the drawbacks associated with it, viz., the fluid needs to be optically transparent and the particle has to be large to be visible. Also, such optical method is likely to fail in case of dense suspensions where the system tends to become more and more opaque. Recently, Fishwick et al.[29] used the positron emission particle tracking (PEPT) to study the hydrodynamics in solid–liquid stirred tanks. They successfully demonstrated that PEPT can provide Lagrangian description of solids hydrodynamics in the reactor, but their study is limited to a very dilute system as well (1% w/w). Also, mostly qualitative information in terms of flow and turbulent kinetic energies in the tank are reported in the article, while quantitative information regarding the particle–liquid slip velocity is only presented for an up-pumping pitched blade turbine. However, in spite of these attempts, the CFD predictions for the solids flow for dense systems have not been evaluated yet and the recent Computer Auto-

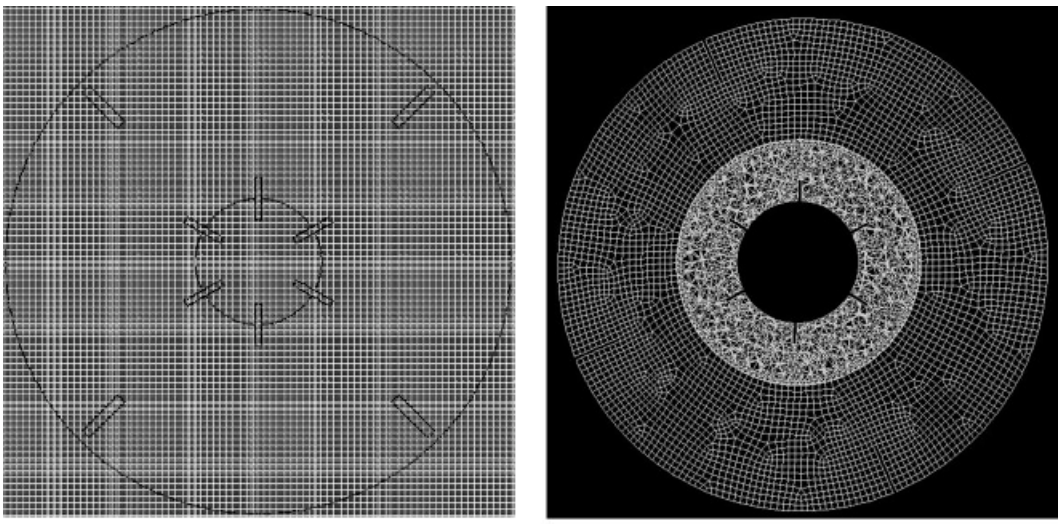

Figure 1. (a) Impeller cross-section showing the grid used for the large eddy simulation, and the points defining the impeller and tank wall via the forcing method; (b) impeller cross-section showing the grid used for the Euler-Euler simulation in Fluent 6.2.

mated Radioactive Particle Tracking (CARPT) experimental studies[30] appears to be a suitable technique for this purpose.

The objective of this work is to assess the quality of predictions obtained from numerical simulations of a complex, turbulent solid–liquid flow in a stirred tank by comparing with results from the CARPT experiment. The focus here is on the dynamic behavior of the dispersed solids phase in terms of solids velocities, turbulent kinetic energy, and solids sojourn times at various parts of the tank. The large eddy simulation and the Euler-Euler model (Fluent 6.2) are the models evaluated in the current work for a solid suspension having overall solids volume fraction of 1% (v/v).

This article is structured as follows. The CARPT technique and the experimental work are summarized first, followed by the details of the LES and the Euler-Euler models used in this study. The next section presents the evaluation of the model results with CARPT data, and finally the work is summarized and conclusions based on the results obtained are made.

Computer Automated Radioactive Particle Tracking Experiment

The computer automated radioactive particle tracking (CARPT) technique maps the flow of solids in the reactor by tracking a single radioactive particle (Sc-46) that has the same size and density as the solids used for the experiment. The instantaneous position of the particle every 0.02 s (50 Hz) is determined from the counts received by an array of scintillation detectors by utilizing the calibration curves that are obtained before the experiment for each of these detectors. These calibration curves are generated by placing the tracer particle at about 500 known locations in different regions of the reactor. The CARPT experiment provides a sequence of instantaneous position data that yields the position of the particle at successive sampling instants. Carrying out a time differentiation of the successive particle positions then provides the instantaneous Lagrangian velocities of the particle. Ensemble averaging of the Lagrangian particle velocities is performed to calculate the average Eulerian velocities of the solids in the system. Fluctuating velocities and solids kinetic energies are also obtained using the mean and instantaneous velocities in the reactor. More details about the CARPT technique can be found elsewhere.[31,32]

The details of the experimental setup and conditions are reported in Guha et al.[30] The reactor consists of a tank of diameter $T = 0.2$ m, the height of liquid (H) being equal to the tank diameter. The agitator is a six-bladed Rushton turbine of diameter $D = T/3$. The distance of the impeller from the bottom of the tank is equal to the impeller diameter. For the experiments, water ($\rho_l = 1000$ kg m^{-3}) was used as the liquid phase and spherical glass beads ($\rho_s = 2500$ kg m^{-3}) of mean diameter 0.3 mm are used as the solids phase. The experimental condition comprised of an overall solids holdup of 1% by volume (2.5% w/w) and an impeller speed of 1000 rpm (or $N = 16.7$ revolutions/s). The Reynolds number then is $Re = ND^2/v = 7.4 \times 10^4$. The just suspended impeller speed based on Zwietering's correlation (1958) for this solid–liquid system is $N_{js} = 15$ revolutions/s.

Modeling Approaches

Large Eddy simulation

The large eddy simulations (LES) are based on an Eulerian-Lagrangian approach. The three-dimensional, unsteady continuous phase flow is solved by means of the lattice-Boltzmann method[33] on a uniform, cubic grid. The grid spacing is such that the diameter of the tank T is spanned by 240 cells [see Figure 1(a)]. The total number of cells considered in the LES is $240^3 \approx 14$ million. The full, three-dimensional geometry of the tank is considered (no assumptions regarding the flow's symmetry have been made). The impeller moves

relative to the fixed grid and the effect of this motion is represented by body forces acting on the fluid. These body forces are adapted dynamically such that at all times the no-slip condition on the impeller surface (shaft, disk, and blades) defined as a collection of closely spaced forcing points not necessarily coinciding with the lattice is satisfied (see Derksen and Van den Akker[14] for a detailed description of this forcing approach). In Figure 1(a) the forcing points have been indicated. The Smagorinsky subgrid-scale model[34] has been used for representing the effect of the unresolved (subgrid) scales on the resolved scales. The Smagorinsky constant C_s was set to 0.1 throughout the flow.

In this flow, spherical solid particles (diameter d_s = 0.3 mm) are dispersed. To get to the desired solids volume fraction of 1% we need to insert some 7 million spheres. The procedure for setting up and solving the equations of motion of the particles has been explained in detail by Derksen.[12] The key features are that for each sphere we solve the equations of linear and rotational motion taking into account drag, (net) gravity, lift forces (being able to determine the Magnus force is the main reason for considering rotational motion of the particles), stress-gradient forces, and added mass. For determining the drag force on the particles, we consider next to the resolved fluid motion also the subgrid-scale motion. The intensity of the latter is estimated via an equilibrium assumption at the subgrid-scales. We subsequently use a Gaussian random process and an eddy-lifetime concept to mimic the fluid motion at the unresolved scales. As in the Euler-Euler approach (see the next section), we consider a nonlinear drag coefficient (according to the Schiller-Naumann model described later).

At the solids volume fractions considered here, particle–particle collisions have great impact on the distribution of solids over the volume of the mixing tank.[12] For this reason, a time-step-driven collision algorithm[35] has been implemented. It keeps track of each individual particle–particle collision in the tank with the restriction (for computational reasons) that one particle can only collide once during one time steps. Given the small time step that we use (we take 2800 time steps per impeller revolution) and the (tank-averaged) solids volume fraction of 1%, the number of collisions that we miss as a result of this restriction is very limited.[12]

The LES results that we present here are all time averaged. After reaching a quasi steady state, the LES was run for a period comprising 16 impeller revolutions to collect sufficient flow information such that converged statistical results could be presented.

Euler-Euler model

The Euler-Euler model available commercially in Fluent 6.2 is the other model evaluated against the experimental data obtained using CARPT. In the Euler-Euler approach, each phase is assumed to coexist at every point in space in the form of interpenetrating continua. It solves the continuity and momentum equations for all the phases present and the coupling between the phases are obtained through pressure and interphase exchange coefficients. For each phase q, the conservation equation is written as a function of the volume fraction of the phase α_q. The continuity equation for phase q without mass transfer between phases is written as

$$\frac{\partial}{\partial t}(\alpha_q \rho_q) + \nabla \bullet (\alpha_q \rho_q \overrightarrow{v_q} - \rho_q D_t \nabla \alpha_q) = 0 \qquad (1)$$

where $\overrightarrow{v_q}$ is the velocity of phase q.

The momentum balances for the liquid and solid phases are respectively

$$\frac{\partial}{\partial t}(\alpha_l \rho_l \overrightarrow{v_l}) + \nabla \bullet (\alpha_l \rho_l \overrightarrow{v_l}\,\overrightarrow{v_l}) = -\alpha_l \nabla p + \nabla \bullet \overline{\overline{\tau_l}} + \alpha_l \rho_l \vec{g} + K_{sl}(\overrightarrow{v_s} - \overrightarrow{v_l}) + \overrightarrow{F_{lift}} \qquad (2)$$

$$\frac{\partial}{\partial t}(\alpha_s \rho_s \overrightarrow{v_s}) + \nabla \bullet (\alpha_s \rho_s \overrightarrow{v_s}\,\overrightarrow{v_s}) = -\alpha_s \nabla p - \nabla p_s + \nabla \bullet \overline{\overline{\tau_s}} + \alpha_s \rho_s \vec{g} + K_{sl}(\overrightarrow{v_l} - \overrightarrow{v_s}) + \overrightarrow{F_{lift}} \qquad (3)$$

The turbulent dispersion of the secondary phase (solids) is accounted in Eq. 1 through the turbulent diffusivity D_t. The default value of 0.75 in Fluent for the dispersion Prandtl number is used in this study to compute the turbulent diffusivity. K_{sl} is the momentum exchange coefficient to account for the interphase drag, while F_{lift} accounts for the lift force between the liquid and the solid phases. The term p_s in Eq. 3 represents the solids pressure which accounts for the force due to particle interactions. This term is closed applying the kinetic theory of granular flow and is composed of a kinetic term and a second term due to particle collisions. The solid pressure is a function of the coefficient of restitution for particle collisions, the granular temperature, and the radial distribution function which corrects for the probability of collisions between grains when the solid phase becomes dense. The granular temperature is proportional to the kinetic energy of the fluctuating particle and is obtained by solving the transport equation derived from the kinetic theory. The default values provided for the granular model constants in the Fluent 6.2 framework are used in the present study, more detailed discussion on which can be found in the Fluent User Manual.[36]

The standard k-ε model with mixture properties is used as the turbulence model. This is based on the observation reported by Montante and Magelli[7] that the mixture model leads to similar results obtained using a k-ε model for each phase while requiring significantly lower computation time. The Multiple Reference Frame (MRF) approach[37] is used to model the rotating impeller, where the flow in the impeller region is solved in a rotating framework while the outer region is solved in a stationary framework. This algorithm assumes the flow to be steady and the impeller-baffle interactions are accounted by suitable coupling at the interface between the two regions where the continuity of the absolute velocity is enforced. The MRF boundary is located at r/R = 0.5 and is in agreement with Oshinowo et al.,[38] which mentions that when the impeller diameter is smaller than half of the tank diameter (which happens to be the case here) the optimal radial position of the boundary between the two zones is roughly midway between the impeller blade tip and the inner radius of the baffle.

The interface exchange coefficient to account for the drag force in Eqs. 2 and 3 involves the drag coefficient C_D and is given by

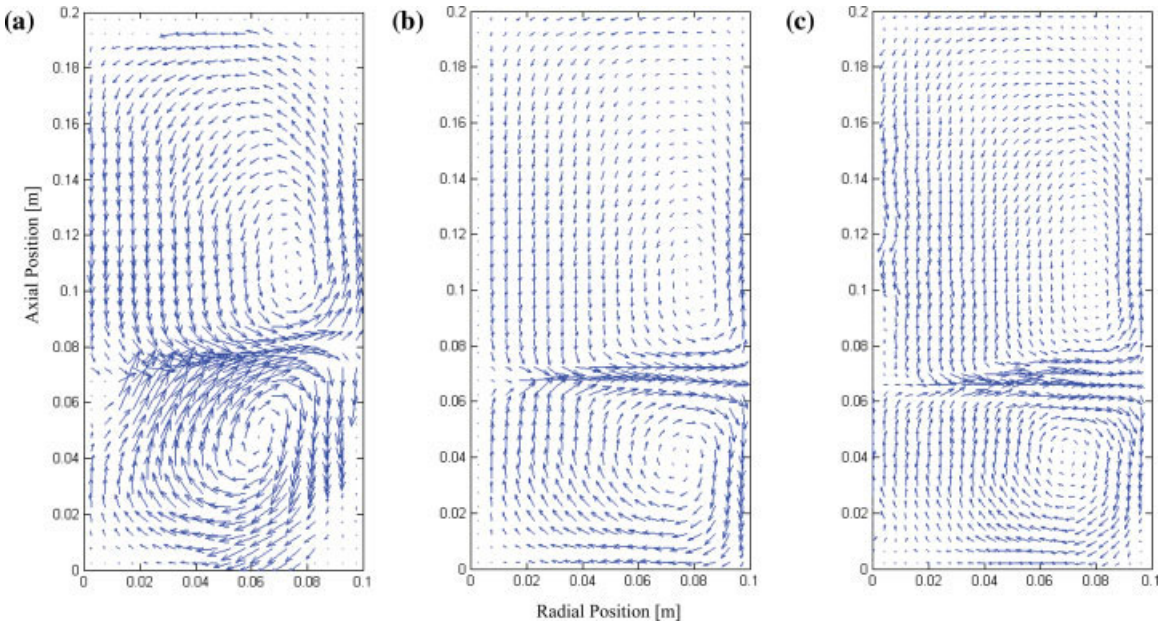

Figure 2. Overall solids flow pattern in the tank as obtained from (a) CARPT, (b) Euler-Euler simulation, and (c) Large Eddy simulation (all figures in same scale).

[Color figure can be viewed in the online issue, which is available at www.interscience.wiley.com.]

$$K_{sl} = \frac{3}{4} C_D \frac{\alpha_s \rho_l |\overrightarrow{v_s} - \overrightarrow{v_l}|}{d_s} \tag{4}$$

In this work, the drag coefficient is quantified using the Schiller-Naumann model,[39] where C_D is obtained as

$$C_D = \begin{cases} 24(1 + 0.15\, Re_s^{0.687})/Re_s & Re_s \leq 1000 \\ 0.44 & Re_s > 1000 \end{cases} \tag{5}$$

Re_s is the relative Reynolds number defined as $Re_s = \frac{\rho_l d_s |\overrightarrow{v_s} - \overrightarrow{v_l}|}{\mu_l}$. The lift force has been shown to have minor influence on the Euler-Euler predictions of solid-liquid flow in a stirred vessel[40] and has been eventually neglected by several authors in their simulations.[7–9] However, it is retained in this work since it was included in the large eddy simulation and is quantified through the lift coefficient C_L, which is kept at the default constant value of 0.5 for the current simulation.

The grid consists of about 589,000 cells consisting of hexahedron and tetrahedron elements as shown in Figure 1(b) to simulate the full geometry of the tank. This grid size is chosen based on a recent study by Khopkar et al.[9] who performed an Euler-Euler simulation in a geometrically similar solid–liquid stirred tank of 0.3 m diameter agitated by a Rushton turbine. They used 287,875 cells to obtain the grid independent solution for the flow in half of the tank. The grid size used in this work is more than twice of that, which is necessary since simulation is performed for the full tank, and considering that the diameter of the tank in this case is smaller than the one simulated by Khopkar et al.,[9] the grid density here is higher than that used in their work. Also, the recent work of Deglon and Meyer[41] for single phase flows in stirred vessels concludes that the mean flow is unaffected by the grid resolution while the turbulent kinetic energy is influenced by the grid density used for the simulation. However, the solids turbulent kinetic energies predicted by the Euler-Euler simulation in this work is compared with those predicted by the large eddy simulation which is significantly more fundamentally based and computed with very high grid resolution (240^3 cells or 13.8 million cells). Since differences in the solids kinetic energy predictions by the two models were minimal throughout the solution domain as shown later in the text, further Euler-Euler simulations with finer grid was not carried out in this work. The Euler-Euler simulation is considered converged when the residuals dropped below 10^{-5}. Also, the overall solids balance is monitored after every iteration to ensure that the solids mass balance is not violated.

Results and Discussion

This section compares the results obtained with the large eddy simulation (LES) and the Euler-Euler model with those obtained from the CARPT experiment. Quantitative comparisons are shown for the mean solids velocity profiles and solids turbulent kinetic energy profiles at four axial regions of the tank that are given by $z/T = 0.075$ (close to the bottom), 0.25 (just below impeller), 0.34 (impeller plane), and 0.65 (midway between impeller and the top free surface). Also, comparison between the predictions of the two models for the liquid phase turbulent kinetic energy, the slip Reynolds number (Re_s) and the solids holdup distribution in the tank are presented and discussed. The mean velocities are made dimensionless with the impeller tip speed, U_{tip}. The turbulent kinetic energy is made dimensionless with U_{tip}^2. The radial location in the tank is non-dimensionalized with the tank radius R ($R = T/2$).

Overall flow pattern

Figures 2(a–c) show the average solids velocity field in a vertical plane in the tank as observed in the CARPT experi-

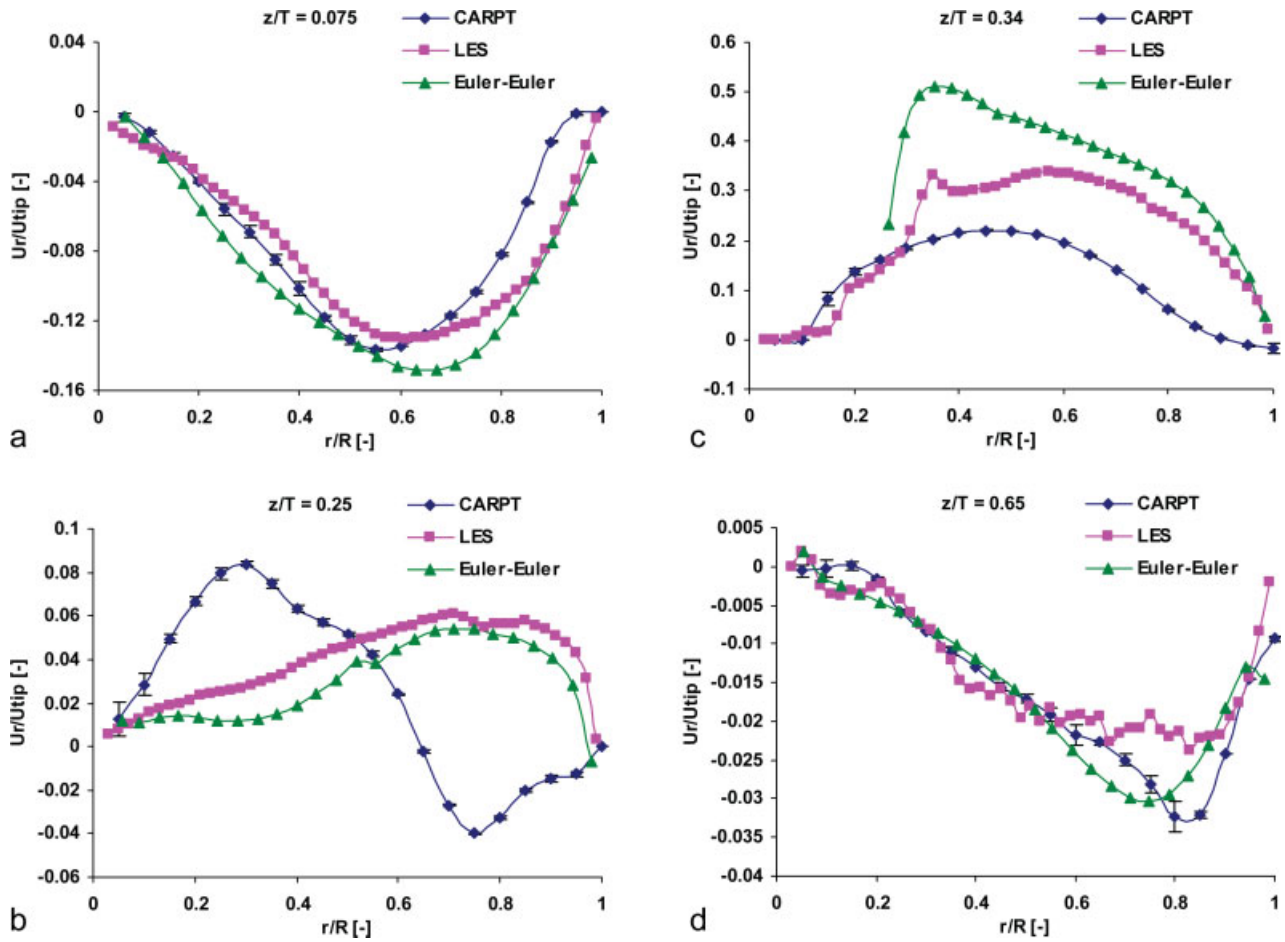

Figure 3. Radial profiles of solids radial velocity at different axial locations in the tank.

[Color figure can be viewed in the online issue, which is available at www.interscience.wiley.com.]

ment and those predicted by the Euler-Euler model and the large eddy simulation, respectively. Clearly, in the experimental result the lower recirculation loop below the impeller is significantly stronger than the one above the impeller. This is not observed in either the large eddy simulation or the Euler-Euler prediction, where qualitatively both loops appear to be equally strong. Also it should be noted that below the impeller near the center where solids flow upward (characteristic flow pattern for radial flow impellers) there is a significant contribution of the radial velocity apart from the strong axial velocity. This is not predicted in the numerical results, where the velocities at those locations are almost completely dominated by the axial component.

Solids velocity radial profiles

The radial profiles of the time (ensemble) averaged solids radial velocity as obtained from the CARPT experiment and the two numerical models at the four axial locations in the reactor are compared in Figures 3(a–d). The Euler-Euler predictions of solids radial velocity are quite comparable with those obtained from the LES simulation, except at the impeller plane ($z/T = 0.34$) where improved predictions compared with CARPT data are observed with LES. However, both models still over-predict the solids velocity in the impeller outstream region. The numerical predictions are reasonably good in the regions far from the impeller and discrepancies are mostly observed in and around the impeller. Just below the impeller, at $z/T = 0.25$ (Figure 3b), both the simulations predict completely different trends from that observed experimentally. This is in line with the observation that was made from the overall flow pattern discussed in the earlier section. The solids flowing upward near the center below the impeller have a stronger radial component as observed in the experimental study than that predicted by the models.

Figures 4(a–d) depict the radial profiles of time (ensemble) averaged solids tangential velocity as obtained from the CARPT experiment and the two numerical models at the four axial locations in the reactor. At the impeller plane ($z/T = 0.34$), the tangential velocity is over-predicted by both the models close to the impeller, but the LES predictions are improved in the region $r/R > \sim 0.4$. At the planes away from the impeller ($z/T = 0.075$ and 0.65), LES predictions of the tangential velocity are far superior to those obtained from the Euler-Euler model particularly in the region $r/R < \sim 0.5$. Although the strong swirl below the impeller plane ($z/T = 0.25$) observed in the experimental data is not captured by any of the models, LES predictions show improved trends compared with its Euler-Euler counterparts throughout the radial domain. Overall, the LES results for the solids tangential

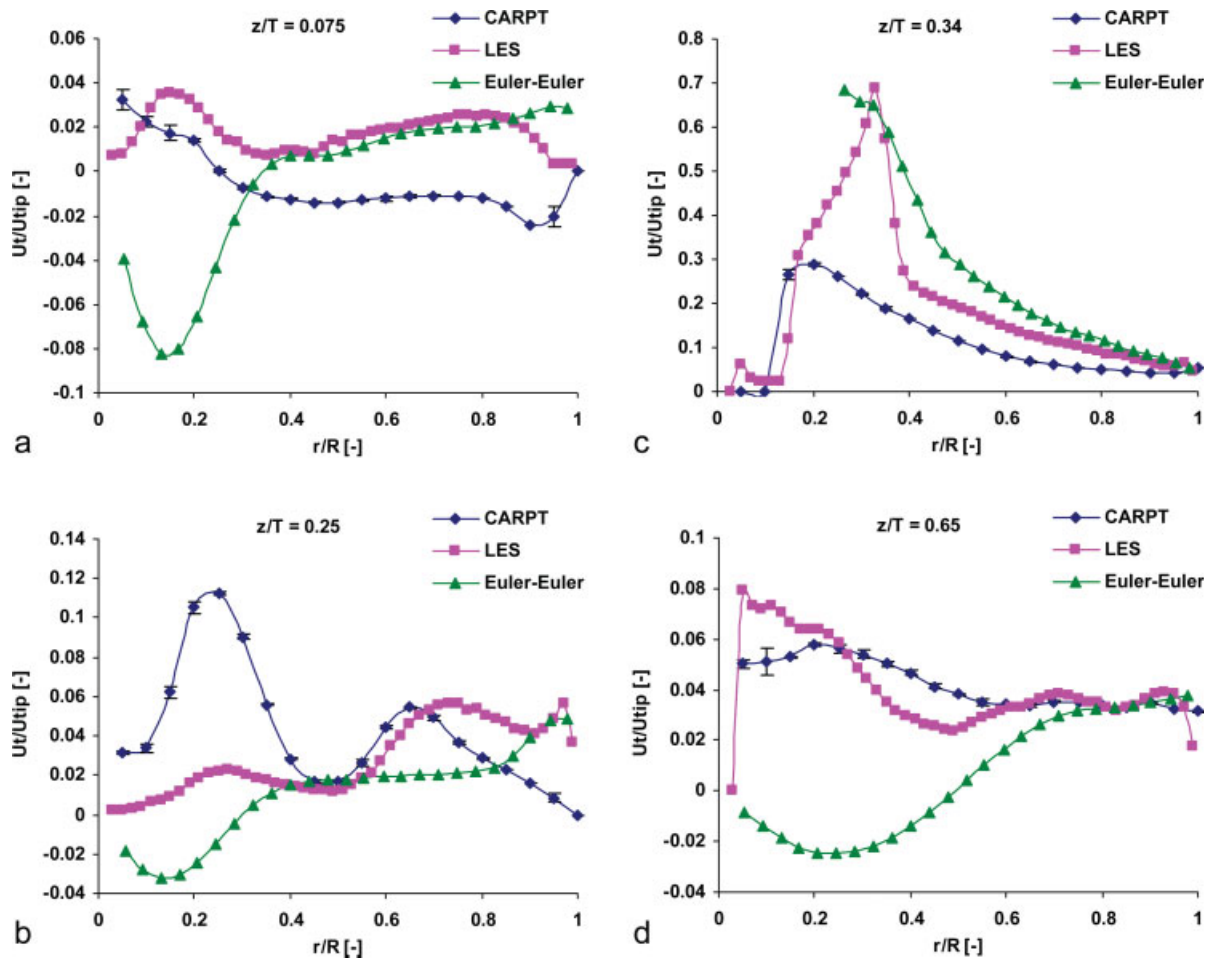

Figure 4. Radial profiles of solids tangential velocity at different axial locations in the tank.

[Color figure can be viewed in the online issue, which is available at www.interscience.wiley.com.]

velocity compare much better with the CARPT experimental findings as opposed to the Euler-Euler predictions, at least in terms of capturing the right trends at all the axial locations presented here.

The radial profiles of solids axial velocity as obtained from the CARPT experiment and the two numerical models at the four axial locations in the reactor are compared in Figures 5(a–d). The predictions obtained with the large eddy simulation and the Euler-Euler model are more or less comparable for the solids axial velocities at most of the axial locations, but improved trend can be observed with the Euler-Euler model in the impeller plane. The numerical results compare reasonably well with the CARPT data (within engineering accuracy) at all the axial planes other than the plane containing the impeller. The solids jet in the impeller stream, as obtained from the experiment, has a significant axial velocity associated with it because of which the jet as a whole slightly moves upward as it approaches the wall. Similar observation is reported by Sbrizzai et al.[16] in their direct numerical simulation of solids dispersion in an unbaffled stirred vessel. The authors attributed the upward inclination of the axis of the jet to the different boundary conditions that are imposed at the bottom (no-slip) and at the top (free-slip) of the tank. However, this cannot be observed in the numerical results obtained in this work using large eddy simulation and the Euler-Euler model.

Turbulent kinetic energy radial profiles

Figures 6(a–d) represent the radial profiles of solids turbulent kinetic energy as obtained from the CARPT experiment and the two numerical models at the four axial locations in the reactor. It is interesting to note that the numerical predictions obtained using the large eddy simulation and the Euler-Euler model are in good agreement at all the four axial locations reported here and no additional improvement in prediction of the solids kinetic energy is observed with the LES model throughout the tank. This is quite surprising since it is well known that LES provides significantly improved predictions of turbulent kinetic energies for single phase flow compared with RANS model.[15] When compared with the CARPT experimental data, it can be observed that the solids turbulent kinetic energies predicted by both the models are over- predicted at the impeller plane and under-predicted at all other axial locations.

It will be of interest to compare the liquid phase turbulent kinetic energies predicted by the two models and to see if both the models provide similar performance. Although the

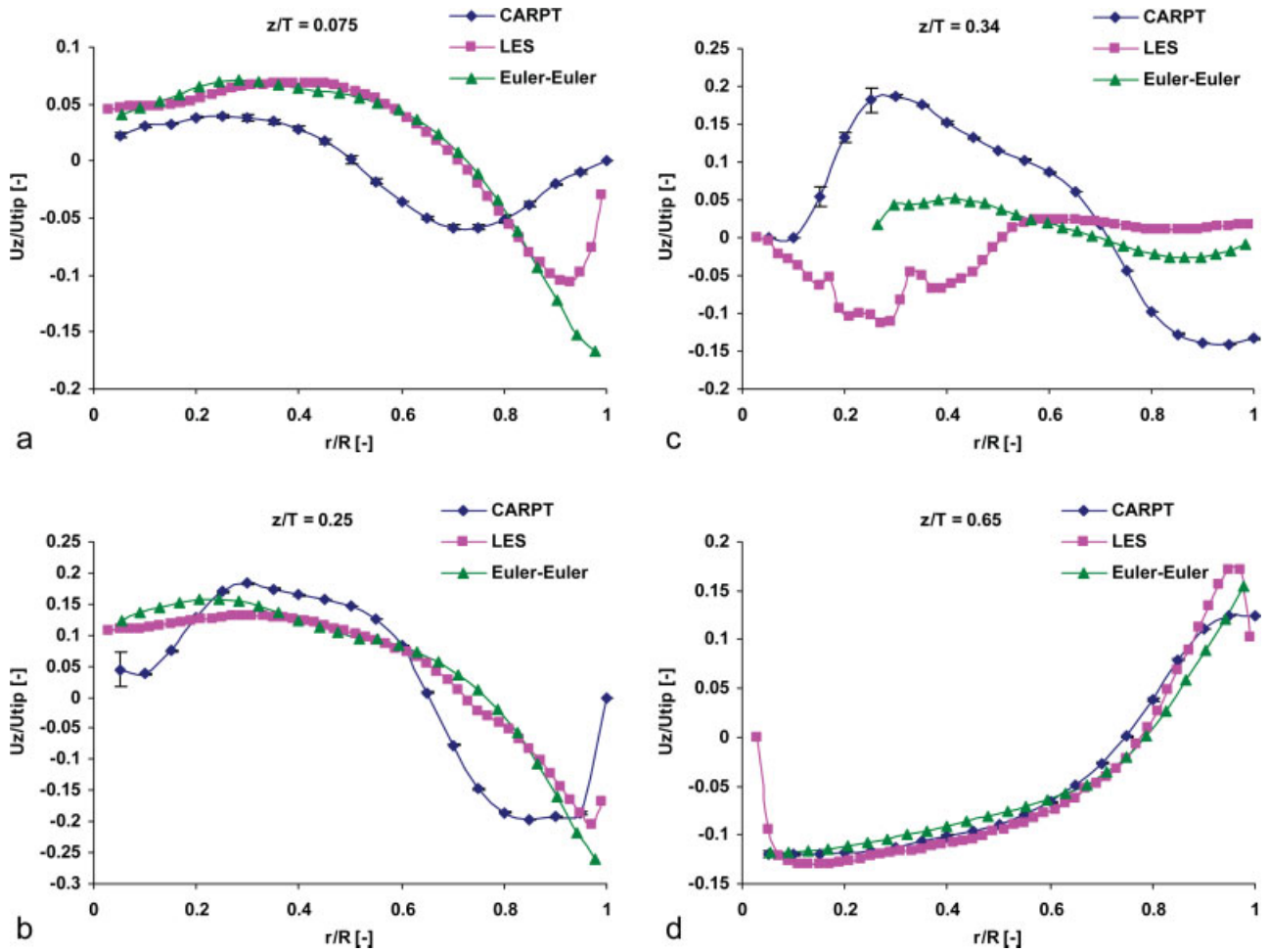

Figure 5. Radial profiles of solids axial velocity at different axial locations in the tank.

[Color figure can be viewed in the online issue, which is available at www.interscience.wiley.com.]

LES model solves for the liquid phase turbulence separately, the Euler-Euler simulation solves for the k-ε model with mixture properties and assumes that the same turbulence field is shared by the two phases. As a result, the mixture turbulent kinetic energy profile obtained from the Euler-Euler model is compared with the liquid phase turbulent kinetic energy obtained from LES at the plane of the impeller ($z/T = 0.34$) in Figure 7. It can be observed that this comparison reveals significant under-prediction of the turbulent kinetic energy from the RANS model compared with those predicted by LES. It seems that the solids phase turbulence might be less sensitive to the model being used while an improved model performs better to resolve the continuous phase turbulence.

Slip Reynolds number

The slip (or relative) Reynolds number (Re_s) quantifies the magnitude of the slip velocity between the two phases in the reactor, and is computed as defined earlier in the text (see below Eq. 5). The lower the value of slip, the more the dispersed phase tends to follow the continuous phase and vice versa. The radial profiles of the slip Reynolds number predicted by the two models at the impeller plane ($z/T = 0.34$) are presented in Figure 8. The slip velocity computed from the Eulerian simulation are significantly lower than those from the large eddy simulation, the difference being more than an order of magnitude at many of the radial locations. The closures used for the inter-phase interactions depend on the computed slip Reynolds number and incorrect quantification of this quantity will affect the simulated flow field significantly.

Solids volume fraction

The radial profiles of the solids holdup (v/v) distribution obtained from the two models are plotted in Figure 9 at the plane containing the impeller ($z/T = 0.34$). Although the qualitative trends are similar, quantitatively LES predicts lower solids holdup compared with Euler-Euler model at most of the radial locations. This is, however, not surprising considering the significantly higher slip Reynolds number predicted by LES (Figure 8). Increased slip leads to more solids to settle down resulting in a lower prediction of solids holdup.

Solids sojourn time distributions

The Lagrangian information obtained from the CARPT experiment and large eddy simulation is used to calculate the

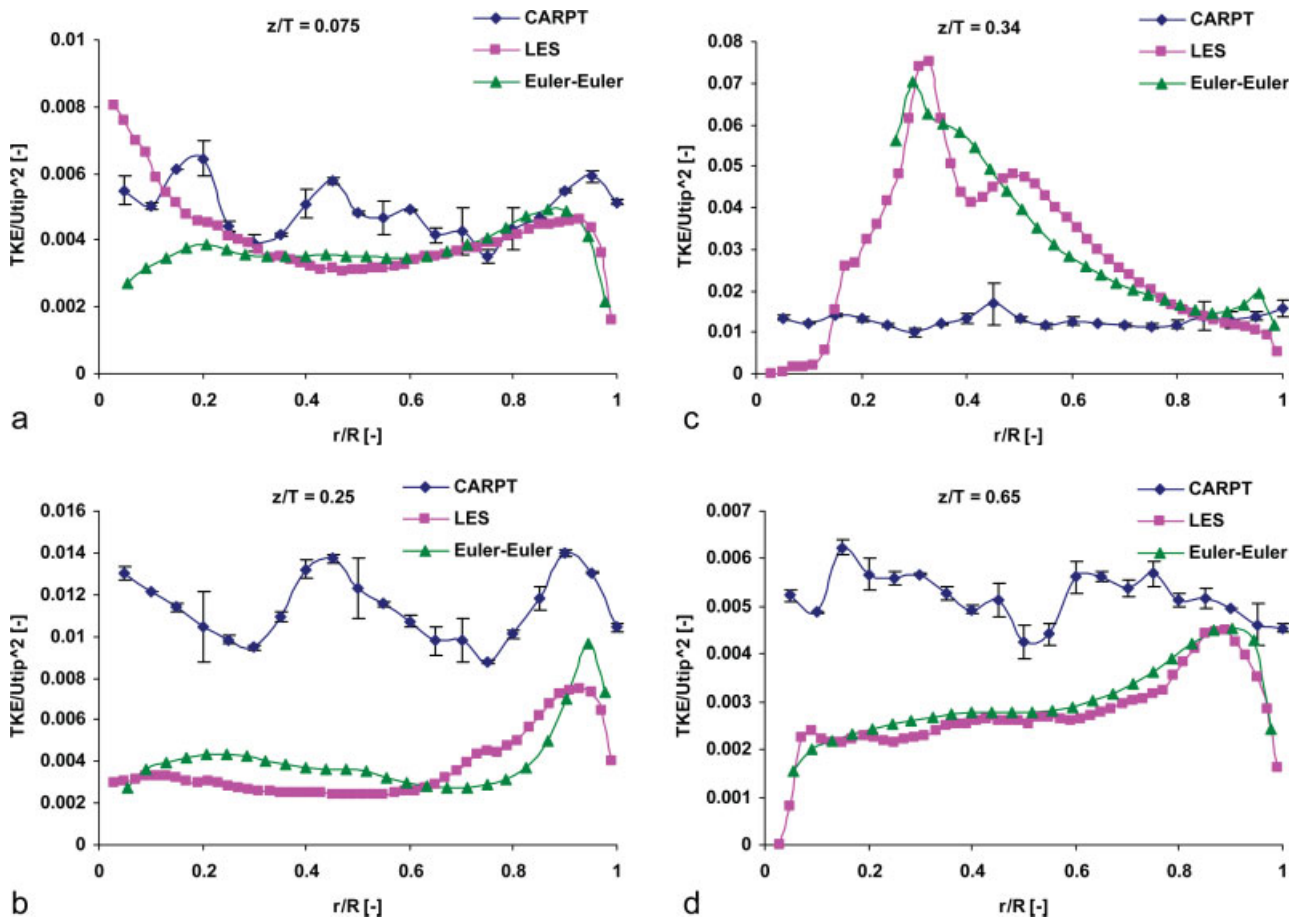

Figure 6. Radial profiles of solids turbulent kinetic energy at different axial locations in the tank.

[Color figure can be viewed in the online issue, which is available at www.interscience.wiley.com.]

probability density function (PDF) of solids sojourn times in different axial regions in the reactor. The concept of solids sojourn time distribution (STD) has been discussed in detail by Guha et al.,[30] where it was used to evaluate the Zwietering's correlation for the "just-suspension" speed for incipient solid suspension in the tank. Based on the mean sojourn time

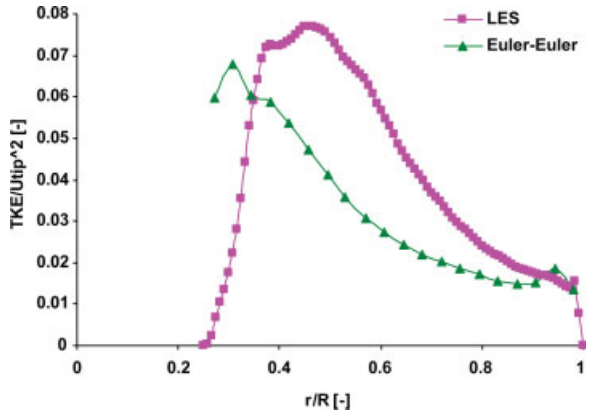

Figure 7. Radial comparison of mixture turbulent kinetic energy from the Euler-Euler model and liquid phase turbulent kinetic energy from the large eddy simulation at the impeller cross-section ($z/T = 0.34$).

[Color figure can be viewed in the online issue, which is available at www.interscience.wiley.com.]

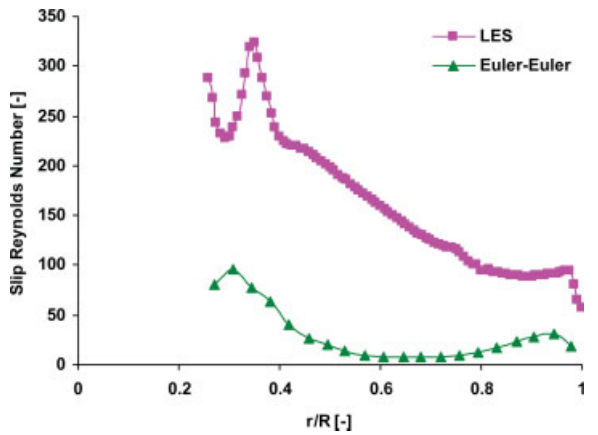

Figure 8. Radial comparison of slip Reynolds number from the Euler-Euler model and the large eddy simulation at the impeller cross-section ($z/T = 0.34$).

[Color figure can be viewed in the online issue, which is available at www.interscience.wiley.com.]

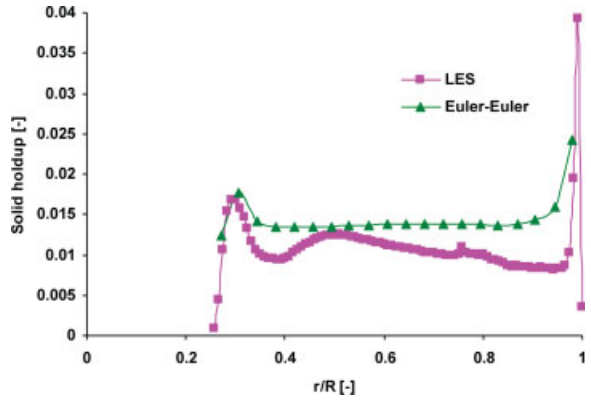

Figure 9. Radial comparison of solids holdup (*v/v*) from the Euler-Euler model and the large eddy simulation at the impeller cross-section (*z/T* = 0.34).

[Color figure can be viewed in the online issue, which is available at www.interscience.wiley.com.]

obtained experimentally for two impeller speeds at the bottom zone of the tank, it was confirmed that the Zwietering's correlation over-predicts the just suspension speed and incipient suspension can be achieved at speeds lower than the "just-suspension" speed predicted by the correlation. This was in line with the observation made by Brucato and Brucato[42] who concluded that practically all particles get suspended at speeds of about 80% of that predicted by the correlation. Reasonable predictions of solids sojourn time distributions in the tank will eventually lead to improved predictions of just-suspension conditions for slurry reactors. From an operational point of view, such optimization of operating condition can result in significant reduction in energy requirement, since the power required scales as the cube of the impeller speed.

To obtain the solids sojourn time distributions (STD), the total height of the tank is divided into 10 equal axial regions (zones) each 2 cm in height and the movement of the tracer particle is monitored across each of these zones. The STD curve in each zone is generated from the particle position vs. time data by recording the time when the particle is found in the zone of interest. Tracking the particle until it exits the zone of interest provides the time the particle spends in the axial zone under consideration from entry to exit. This yields the sojourn time of the particle in the zone of interest during that pass. This process is repeated each time the particle enters and leaves the zone under consideration, which then provides a distribution of sojourn times of the particle in that axial region. Therefore, the sojourn time distribution (STD) in any axial zone i can be defined as

$E_i(t_s)\Delta t_s$ = fraction of occurrences in zone i that has sojourn times between t_s and $t_s + \Delta t_s$

The moments of the STDs are calculated in order to characterize the obtained distributions. The first moment provides the mean of the distribution η_i, which is defined as

$$\eta_i = \sum_{t_s=0}^{\infty} t_s E_i(t_s)\Delta t_s \tag{6}$$

The second central moment gives the variance of the distribution σ_i^2, which is defined as

$$\sigma_i^2 = \sum_{t_s=0}^{\infty} (t_s - \eta_i)^2 E_i(t_s)\Delta t_s \tag{7}$$

The positive square-root of the variance is the standard deviation of the distribution, which depicts how much the distribution spreads out with respect to the mean value.

The axial variation of the mean and standard deviation of the solids sojourn time distributions in the tank as obtained from the CARPT experiment and the large eddy simulation is compared in Figures 10(a, b). The sojourn time distributions cannot be obtained with the Euler-Euler model since the dynamics of the solids phase is also solved in the Eulerian framework, unlike the large eddy simulation which tracks the individual particles through a Lagrangian approach. It can be seen that the first and second moments of the distributions predicted by LES compare well with those from CARPT experiment, both qualitatively and quantitatively, in spite of the fact that significant mismatch between CARPT results and LES predictions of velocities are observed particularly around the impeller. This is somewhat surprising considering that one would expect the mismatch in the velocity

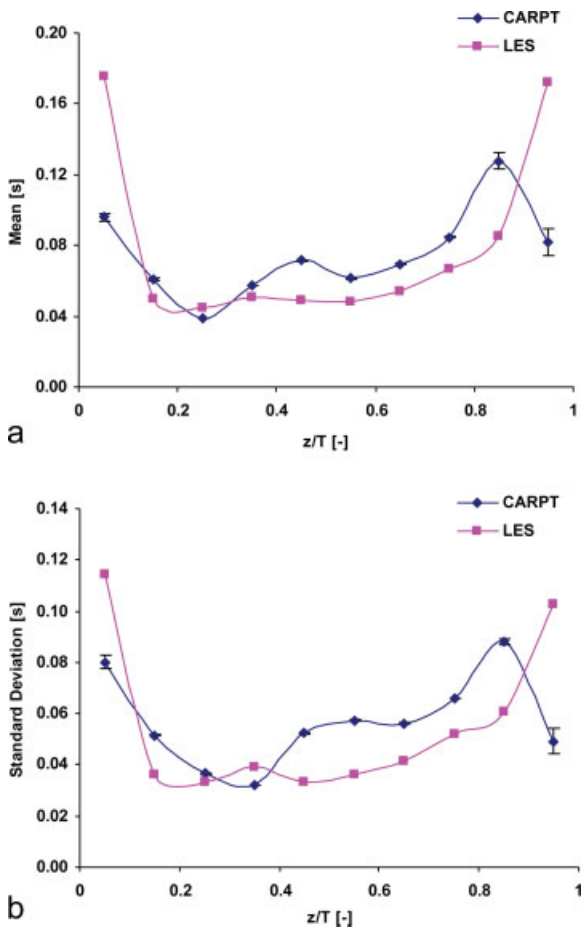

Figure 10. Axial variation of the moments of the solids sojourn time distribution in the tank.

[Color figure can be viewed in the online issue, which is available at www.interscience.wiley.com.]

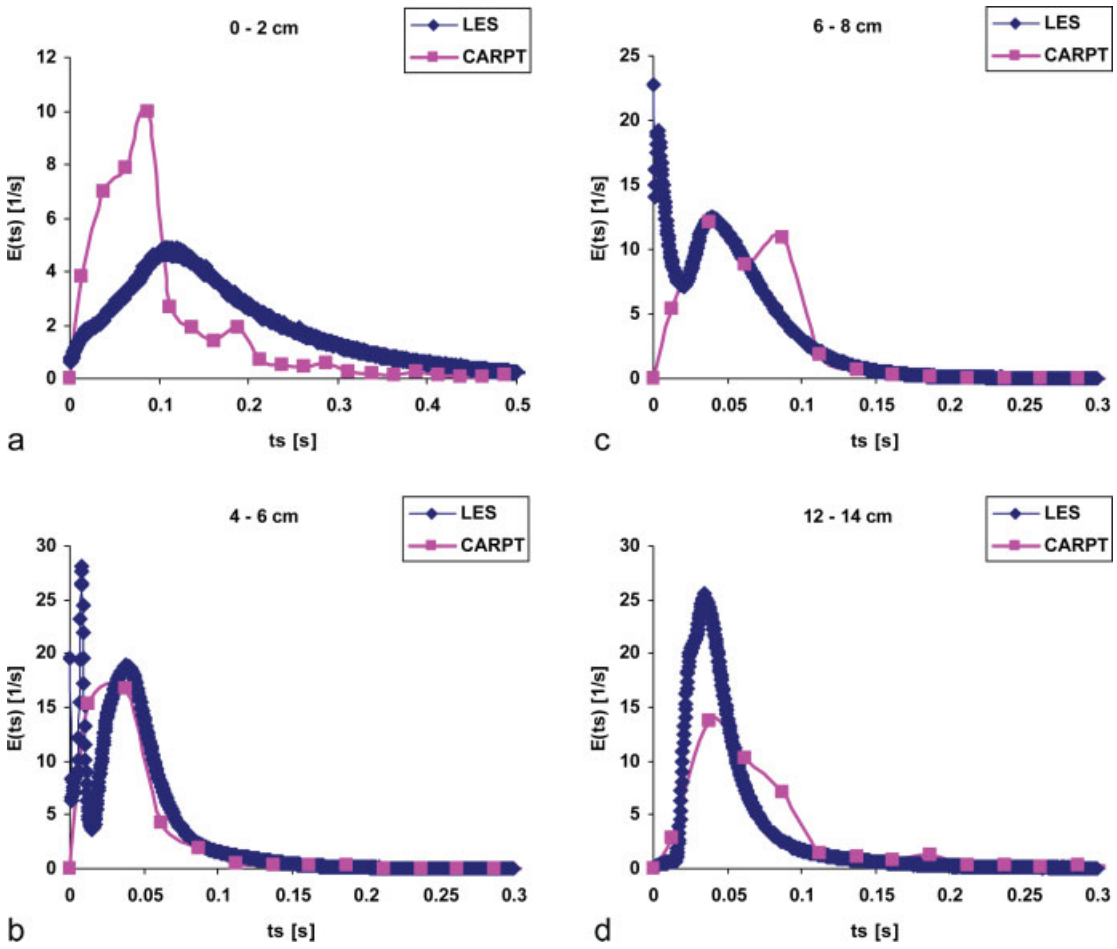

Figure 11. Solids sojourn time distributions at different axial slices in the tank.

[Color figure can be viewed in the online issue, which is available at www.interscience.wiley.com.]

profiles to be reflected in the sojourn time distributions as well. As a result it is worthwhile to compare the distribution functions obtained from CARPT data and the LES simulation at four axial slices containing the four axial locations where the velocity profiles are compared. Such a comparison is presented in Figures 11(a–d), where the slices considered are 0–2 cm (containing $z/T = 0.075$), 4–6 cm (containing $z/T = 0.25$), 6–8 cm (containing $z/T = 0.34$), and 12–14 cm (containing $z/T = 0.65$). The PDF obtained for the bottom slice by the two methods is characteristically different—CARPT shows a larger fraction having small sojourn time compared to LES prediction, and hence the mean sojourn time predicted by LES is larger for this slice. For the slice just below the impeller (4–6 cm), significant difference in the PDF can be observed qualitatively. The spike predicted by the large eddy simulation is not observed by CARPT. However, this spike will have less impact on the first and second moments of the distribution since the spike occurs at very small t_s, which probably led to similar mean and standard deviation for the two cases. In the axial slice containing the impeller (6–8 cm) both CARPT and LES show two peaks but the peaks are slightly shifted toward the left with LES compared with that with CARPT. The range of sojourn time (t_s) covered by the distribution is, however, more or less equal. Significant difference in the PDF exists for the slice between 12 and 14 cm as well, but the two distributions lead to similar first moment (mean) although the second moment (standard deviation) obtained from CARPT is larger.

Summary and Conclusions

In this work, the ability of the large eddy simulation (LES) and the Euler-Euler CFD model in predicting the solids dynamics in a solid-liquid stirred tank reactor is evaluated through an extensive qualitative and quantitative comparison of the solids phase velocities, turbulent kinetic energy, and sojourn time distributions (STD) with those obtained using computer automated radioactive particle tracking (CARPT) experiment. The overall flow pattern obtained using the CARPT technique shows the bottom recirculation loop to be significantly stronger than the top one, which is not captured by either the large eddy simulation or the Euler-Euler model. The predictions of the azimuthally averaged velocity components, particularly the tangential component, at different axial locations in the reactor are improved when LES is used as compared with the Euler-Euler model. Major discrepancies in the prediction of solids velocities by the numerical models can be seen in and around the impeller plane. In spite of the observed mismatch in time-averaged velocity predictions compared with CARPT data, the large eddy simulation

provides reasonably good agreement for the mean and standard deviation of the solids sojourn times in the reactor with the experimentally determined values. Based on the observations presented in this work, it can be concluded that more fundamental understanding of the flow field and the associated interactions close to the impeller are necessary to resolve and predict the complex two-phase flow in a solid–liquid stirred tank reactor. However, reasonable predictions of LES for the mean and variance of the sojourn time distributions in various zones of the tank provides additional encouragement for extending the compartmental model for the stirred tank reactor to liquid–solid systems. In such models for single phase flow,[43] the CFD computed flow field is used to couple the compartmental model with kinetics of the desired reaction system.

Acknowledgments

This work was partly supported by the NSF-ERC award (EEC-0310689) from the National Science Foundation Engineering Research Centers Program through the Center for Environmentally Beneficial Catalysis (CEBC). Industrial sponsors of Chemical Reaction Engineering Laboratory (CREL) at Washington University in St. Louis are also greatly acknowledged.

Notation

C = impeller clearance
d_s = particle diameter
C_D, C_L = drag and lift coefficient
D = impeller diameter
E = sojourn time distribution
R = tank radius
t_s = solids sojourn time
T = tank diameter
v = velocity
U_{tip} = impeller tip speed
ρ = density
α = volume fraction
μ = viscosity
η = mean of sojourn time distribution
σ = standard deviation of sojourn time distribution
Re_s = relative (slip) Reynolds number

Literature Cited

1. Gosman AD, Lekakou C, Politis S, Issa RI, Looney MK. Multidimensional modeling of turbulent two-phase flows in stirred vessels. *AIChE J*. 1992;38:1946.
2. Barrue H, Bertrand J, Cristol B, Xuereb C. Eulerian simulation of dense solid-liquid suspension in multi-stage stirred vessel. *J Chem Eng Japan*. 2001;34:585.
3. Altway A, Setyawan H, Margono, Winardi S. Effect of particle size on simulation of three-dimensional solid dispersion in stirred tank. *Trans IChemE*. 2001;79(A):1011.
4. Montante G, Micale G, Magelli F, Brucato A. Experiments and CFD predictions of solid particle distribution in a vessel agitated with four pitched blade turbines. *Trans IChemE*. 2001;79(A):1005.
5. Sha Z, Palosaari S, Oinas P, Ogawa K. CFD simulation of solid suspension in a stirred tank. *J Chem Eng Japan*. 2001;34:621.
6. Micale G, Grisafi F, Rizzuti L, Brucato A. CFD simulation of particle suspension height in stirred vessels. *Trans IChemE*. 2004;82(A):1204.
7. Montante G, Magelli F. Modeling of solids distribution in stirred tanks: analysis of simulation strategies and comparison with experimental data. *Int J Comput Fluid Dynamics*. 2005;19:253.
8. Spidla M, Mostek M, Sinevic V, Jahoda M, Machon V. Experimental assessment and CFD simulations of local solid concentration profiles in a pilot-scale stirred tank. *Chem Pap*. 2005;59(6a):386.
9. Khopkar AR, Kasat GR, Pandit AB, Ranade VV. Computational fluid dynamics simulation of the solid suspension in a stirred slurry reactor. *Ind Eng Chem Res*. 2006;45:4416.
10. Decker S, Sommerfeld M. Calculation of particle suspension in agitated reactors with the Euler-Lagrange approach. *IChemE Symp Ser*. 1996;140:71.
11. Zhang X, Ahmadi G. Eulerian-Lagrangian simulations of liquid-gas-solid flows in three-phase slurry reactors. *Chem Eng Sci*. 2005;60:5089.
12. Derksen JJ. Numerical simulation of solids suspension in a stirred tank. *AIChE J*. 2003;49:2700.
13. Davidson PA. *Turbulence—An Introduction for Scientists and Engineers*. New York: Oxford University Press, 2004.
14. Derksen JJ, Van den Akker HEA. Large eddy simulations on the flow driven by a rushton turbine. *AIChE J*. 1999;45:209.
15. Hartmann H, Derksen JJ, Montavon C, Pearson J, Hamill IS, Van den Akker HEA. Assessment of large eddy and RANS stirred tank simulations by means of LDA. *Chem Eng Sci*. 2004;59:2419.
16. Sbrizzai F, Lavezzo V, Verzicco R, Campolo M, Soldati A. Direct numerical simulation of turbulent particle dispersion in an unbaffled stirred-tank reactor. *Chem Eng Sci*. 2006;61:2843.
17. Nienow AW. Suspension of solid particles in turbine-agitated, baffled vessels. *Chem Eng Sci*. 1968;23:1453.
18. Takahashi K, Fujita H. A study of the agitation speed to just cause complete suspension for non-spherical particles. *J Chem Eng Japan*. 1995;28:237.
19. Armenante PM, Nagamine EU, Susanto J. Determination of correlations to predict the minimum agitation speed for complete solid suspension in agitated vessels. *Can J Chem Eng*. 1998;76:413.
20. Wu J, Zhu Y, Pullum L. Impeller geometry effect on velocity and solids suspension. *Trans IChemE*. 2001;79(A):989.
21. Zwietering THN. Suspending of solid particles in liquid by agitators. *Chem Eng Sci*. 1958;8:244.
22. Yamazaki H, Tojo K, Miyanami K. Concentration profiles of solids suspended in a stirred tank. *Powder Technol*. 1986;48:205.
23. Barresi A, Baldi G. Solid dispersion in an agitated vessel. *Chem Eng Sci*. 1987;42:2949.
24. Shamlou PA, Koutsakos E. Solids suspension and distribution in liquids under turbulent agitation. *Chem Eng Sci*. 1989;44529.
25. Godfrey JC, Zhu JM. Measurement of particle-liquid profiles in agitated tanks. *AIChE Symp Ser*. 1994;299:181.
26. Micale G, Montante G, Grisafi F, Brucato A, Godfrey J. CFD simulation of particle distribution in stirred vessels. *Trans IChemE*. 2000;78(A):435.
27. Nouri JM, Whitelaw JH. Particle velocity characteristics of dilute to moderately dense suspension flows in stirred reactors. *Int J Multiphase Flow*. 1992;18:21.
28. Wittmer S, Vivier H, Falk L, Villermaux J. Characterization of mixing by analysis of particle trajectories. *Récents Progrès Génie Procédés*. 1997;11:35.
29. Fishwick R, Winterbottom M, Parker D, Fan X, Stitt H. The use of positron emission particle tracking in the study of multiphase stirred tank reactor hydrodynamics. *Can J Chem Eng*. 2005;83:97.
30. Guha D, Ramachandran PA, Dudukovic MP. Flow field of suspended solids in a stirred tank reactor by Lagrangian tracking. *Chem Eng Sci*. 2007;62:6143.
31. Chaouki J, Larachi F, Dudukovic MP. *Non-Invasive Monitoring of Multiphase Flows*. Amsterdam: Elsevier, 1997.
32. Larachi F, Chaouki J, Kennedy G, Dudukovic MP. *Radioactive Particle Tracking in Multiphase Reactors: Principles and Applications*, *Noninvasive monitoring of multiphase flows*, Chapter 11. Amsterdam: Elsevier, 1997:335.
33. Chen S, Doolen GD. Lattice Boltzmann method for fluid flows. *Annu Rev Fluid Mech*. 1998;30:329.
34. Smagorinsky J. General circulation experiments with the primitive equations, Part 1: the basic experiment. *Mon Weather Rev*. 1963;91:99.
35. Chen M, Kontomaris K, McLaughlin JB. Direct numerical simulation of droplet collisions in a turbulent channel flow, Part I: collision algorithm. *Int J Multiphase Flow*. 1998;24:1079.

36. Fluent User Manual. Lebanon: Fluent Inc. Available at: http://www.fluentusers.com/fluent6326/doc/doc_f.htm. July 2007.
37. Ranade VV. *Computational Flow Modeling for Chemical Reactor Engineering*. New York: Academic Press, 2002.
38. Oshinowo L, Jaworski Z, Dyster KN, Marshall E, Nienow AW. Predicting the tangential velocity field in stirred tanks using the multiple reference frames (MRF) model with validation by LDA measurement. *In the 10th European Mixing Conference*. Amsterdam: Elsevier, 2000:281.
39. Schiller L, Naumann A. Uber die grundlegenden berechungen bei der schwer kraftaufbereitung. *Verein Deutscher Ingenieure*. 1933;77:318.
40. Ljungqvist M, Rasmuson A. Numerical simulation of the two-phase flow in an axially stirred vessel. *Trans IChemE*. 2001;79(A):533.
41. Deglon DA, Meyer CJ. CFD modeling of stirred tanks: numerical considerations. *Minerals Eng*. 2006;19:1059.
42. Brucato A, Brucato V. Unsuspended mass of solid particles in stirred tanks. *Can J Chem Eng*. 1998;76:420.
43. Guha D, Dudukovic MP, Ramachandran PA, Mehta S, Alvare J. CFD-based compartmental modeling of single phase stirred tank reactors. *AIChE J*. 2006;52:1836.

Manuscript received Mar. 29, 2007, and revision received Nov. 20, 2007.